

Comparative analysis of growth, biomass and antioxidative responses in microalgae: a study of *Chlorella vulgaris*, *Isochrysis galbana* and *Tetraselmis chui* across growth phases

Norhayati Yusuf  . Nurul Shafiq Yusof . Malinna Jusoh

Received: 17 July 2024 / Accepted: 24 October 2024 / Published online: 30 October 2024
© The Author(s) 2020

Abstract Microalgae are a promising source of natural antioxidants, but optimising culture conditions to enhance antioxidant production remains a significant challenge, as varying cultivation environments induce oxidative stress and promote antioxidant accumulation. This study aims to assess the production of enzymatic (superoxide dismutase, SOD; catalase, CAT; ascorbate peroxidase, APX; guaiacol peroxidase, GPX; glutathione reductase, GR) pigments and non-enzymatic antioxidants (chlorophylls, Chls; carotenoids, CAR; ascorbic acid, AsA; α -tocopherol, TOC; total glutathione, GSH) in *Chlorella vulgaris* (UMT-M1), *Isochrysis galbana* (SWC002), and *Tetraselmis chui* (SWC001) at different growth phases. Throughout the cultivation period, the early stationary phase was observed to be the most significant increase phase for most antioxidants. All tested species formed TOC in the largest amounts during this phase. In this phase, *C. vulgaris* and *I. galbana* had the highest CAT and GPX, whereas *C. vulgaris* and *T. chui* had the highest SOD and APX. By identifying the early stationary phase as a key growth phase for maximum antioxidant production, this research provides valuable insights into the cultivation strategies that can be employed to maximise the yield of these beneficial compounds. This study thus contributes to the growing body of knowledge necessary for commercialising microalgae-derived antioxidants, offering a sustainable and natural alternative to synthetic antioxidants.

Keywords Antioxidants . Culture conditions . Growth phases . Microalgae . Oxidative

Introduction

Microalgae are rich in nutritious components such as protein, lipids, carbohydrates, vitamins, and minerals, although their composition varies significantly depending on species and environmental variables. Microalgae typically contains 50–70% protein as part of their composition, over 50% carbohydrates in their dry weight, and up to 70% lipid content in oleaginous species, which account for 30–50% of the total weight (Reitan et al. 2021). These nutritional contents can be regulated by manipulating the microalgal growth conditions. Nitrogen depletion, high salinity, high temperature, and pH alteration are the common manipulations to upsurge lipid production. In addition, microalgae excel at producing nutritious polyunsaturated fatty acids, including eicosapentaenoic acid (EPA) and docosahexaenoic acid (DHA), when subjected to salinity stress, nutrient limitations, or light adjustments. These fatty acids from microalgae can serve as an alternative resource, helping to mitigate the depletion of ocean fish (Sharma et al. 2020).

Norhayati Yusuf (✉) . Malinna Jusoh
Faculty of Science and Marine Environment, Universiti Malaysia Terengganu, 21030 Kuala Nerus, Terengganu, Malaysia
Biological Security and Sustainability Research Interest Group (BIOSES), Universiti Malaysia Terengganu, 21030 Kuala Nerus, Terengganu, Malaysia
e-mail: yatiusuf@umt.edu.my

Nurul Shafiq Yusof
SATREPS-COSMOS Laboratory, Centre of Research and Field Service, Universiti Malaysia Terengganu, 21030 Kuala Nerus, Terengganu, Malaysia
Institute of Climate Adaptation and Marine Biotechnology (ICAMB), Universiti Malaysia Terengganu, 21030 Kuala Nerus, Terengganu, Malaysia

Microalgae are rich in natural pigments like carotenoids, chlorophylls, and phycobiliproteins. Pigments refer to intricate molecules or macromolecules capable of changing the colour of light that they transmit or reflect through selective absorption of specific wavelengths. In microalgae, natural pigments serve a crucial function in various activities reliant on pigmentation, including mechanisms related to photosynthesis. These pigments commonly exhibit antioxidant, anticancer, antiviral, and anti-inflammatory properties, which benefit the cosmetics, pharmaceutical, and food industries. Lipid-soluble chlorophylls, the primary photosynthetic pigments, have been utilised in the food industry and pharmaceutical products as natural colourants (Manzoor et al. 2024).

Among the microalgae attracting significant biotechnological interest are *Chlorella spp.*, *Tetraselmis spp.*, *Isochrysis spp.*, *Nannochloropsis spp.*, *Pavlova spp.*, and *Thalassiosira spp.*. These species are increasingly recognised as valuable sources of natural antioxidants due to their rich content of encapsulated bioactive compounds, including both primary and secondary metabolites. They have diverse applications across health food, bioenergy, nutraceutical, and pharmaceutical sectors and serve as animal feed in industries such as aquaculture, agriculture, and pets (Ahmad et al. 2020).

In this study, *C. vulgaris*, *I. galbana*, and *T. chui* were selected for their high nutritional content and antioxidant properties, highlighting their potential in aquaculture, nutraceuticals, and biofuel production, making them significant subjects for ongoing research in biotechnology and nutrition. *C. vulgaris* exhibits exceptional resilience to varying environmental conditions, including changes in light intensity, temperature, and nutrient availability, allowing it to thrive in diverse aquatic environments, in natural and controlled settings (Su et al. 2023). Its rapid growth rate further enhances its robustness, facilitating efficient biomass production crucial for commercial applications. This microalga is rich in bioactive compounds, including vitamins A, C, and E, and carotenoids, contributing to its antioxidant properties. These antioxidants are vital for combating oxidative stress by neutralising free radicals and protecting cellular components from damage. Consequently, the combination of its robustness and high antioxidant content makes *C. vulgaris* a promising candidate for applications in health foods, nutraceuticals, and as a supplement in aquaculture (Udayan et al. 2023).

I. galbana is renowned for its high nutritional value, particularly as a source of essential fatty acids, antioxidants, and pigments. This species is rich in polyunsaturated fatty acids, especially omega-3 and omega-6 fatty acids, which are critical for human health and commonly used in aquaculture and fish farming. It typically contains 20–30% lipid content, with a significant portion comprising highly beneficial unsaturated fats (Sánchez-Bayo et al. 2020). Additionally, *I. galbana* possesses various antioxidants, including carotenoids like fucoxanthin and vitamins, contributing to its ability to mitigate oxidative stress. These compounds enhance the nutritional profile of the algae and promote the health and growth of aquatic animals when included in their feed (Rahman et al. 2020). *T. chui* is another promising microalga known for its adaptability and high nutritional value, containing 35 to 40% proteins, 30 to 35% carbohydrates, and 5 to 10% fats. It is also a good producer of fat-soluble carotenoids, which can serve as supplements for enhancing fish flesh and egg pigmentation (Khatoon et al. 2018). Furthermore, due to its robust growth and high nutritional profile, *T. chui* has been studied for its potential in bioremediation and biofuel production, as well as its applications in aquaculture.

During cultivation, microalgae pass through four different development phases consisting of lag (no or little growth), exponential (rapid growth), stationary (steady growth), and death (lysis). During the lag or induction phase, an initial defer in growth with no or a little increase in the number of cells is observed. This initial period is important for microalgae as a physiological adaptation toward new environmental conditions. In this phase, new cellular components for metabolism and growth are synthesised (Chowdury et al. 2020). After the lag phase, cells enter the exponential or log phase. Metabolic activity is high as DNA, RNA, cell components, and other substances necessary for growth are generated for division. The cell numbers are rapidly increasing and actively divided in the presence of nutrients and optimal light intensity. However, the cell division depends primarily on species, light quantity, and temperature (Zachleder et al. 2021). Eventually, the rapid population growth observed during the log phase begins to decline as available nutrients are depleted and waste products accumulate. Microalgae cell growth then reaches a plateau, known as the stationary phase, where the number of dividing cells equals the number of dying cells, resulting in no net population growth. Under less favourable conditions, competition for nutrients intensifies, decreasing cell metabolic activity. During the death phase, the number of living



cells decreases exponentially, and population growth experiences a sharp decline due to reduced nutrient availability, pH changes, contamination, and waste accumulation (Chowdury et al. 2020).

The synthesis of microalgal antioxidants is commonly appreciable in the growth stages as an adaptive response to oxidative stress. Throughout the growth phases, reactive oxygen species (ROS) are produced in microalgae as metabolic by-products, and exponential and stationary phases have been reported with higher ROS accumulation (Ugya et al. 2019), thus leading to the interactive regulation of natural antioxidants to counteract the harmful ROS. Among the ROS are the free radicals like superoxide radical ($O_2^{\cdot-}$) and hydroxyl radical ($\cdot OH$), as well as non-radical forms like hydrogen peroxide (H_2O_2) and singlet oxygen (1O_2) (Shi et al. 2020). Among them, $\cdot OH$ is a very reactive ROS in connection with chemical activity as it can oxidise most organic molecules, while H_2O_2 is moderately reactive. High ROS accumulation in cells will trigger oxidative stress, which may impair the macromolecules such as lipids, proteins and DNA (Ugya et al. 2019).

Microalgae activate antioxidant pathways to mitigate oxidative damage by ROS. The major group of antioxidants in microalgae is carotenoids (CAR), but there are also significant amounts of other antioxidants such as superoxide dismutase (SOD), catalase (CAT), peroxidase (POD) and glutathione reductase (GR) as well as low molecular weight antioxidants, i.e. ascorbic acid (AsA), tocopherols (TOC) and glutathione (GSH) (Zhang et al. 2020; Hasanuzzaman et al. 2020). SOD is a primary defence antioxidant that catalyses the dismutation of $O_2^{\cdot-}$ to H_2O_2 and oxygen (O_2). H_2O_2 produced needs to be further detoxified by CAT and PODs to water (H_2O) and O_2 . AsA, GSH, and TOC played interrelated roles in significantly limiting ROS production (Zhang et al. 2020).

Current research on microalgae primarily focuses on specific growth phases, highlighting a significant gap in understanding the antioxidative mechanisms throughout all growth stages. This study addresses this gap by investigating the growth, biomass, and responses of enzymatic and non-enzymatic antioxidants in *C. vulgaris*, *I. galbana*, and *T. chui* across different growth phases of microalgae. Understanding these mechanisms is crucial as it may provide insights into optimising cultivation conditions to enhance antioxidant production, which is vital for various applications in health foods, nutraceuticals, and aquaculture. Additionally, results obtained in this study can help future strategies for biotechnological applications, including biofuel production and bioremediation, thereby supporting sustainable practices in these fields.

Materials and methods

Cultural Initiation and cultivation *Chlorella vulgaris* (UMT-M1), *Isochrysis galbana* (SWC002), and *Tetraselmis chui* (SWC001) cultures were obtained from the Institute of Climate Adaptation and Marine Biotechnology (ICAMB), Universiti Malaysia Terengganu, Kuala Nerus, Terengganu, Malaysia. The first step in cultural initiation is inoculation, where a small amount of the selected microalgae cells from a pre-existing stock culture obtained from ICAMB is introduced into a fresh medium. The inoculums of each species were cultivated in 500 mL conical flasks containing 450 mL of filtered-sterilized seawater at 30 ppt salinity and pH 8.0 ± 0.2 enriched with F/2 medium (Guillard 1975). The cultures were incubated under continuously 2,000 lux of 6,500 K daylight white LED lamps as a light source at a constant temperature of $24 \pm 2^\circ C$ in a growth chamber. The aeration was supplied with a Hailea HAP-120 pump (Hailea Group Co., China) with an airflow rate of around 120 L/min of air under the pressure of 0.018 MPa and filtered through 0.22 μm Minisart Sartorius syringe filter to avoid contamination. All species were initially cultured from an equal inoculum at 1×10^6 cells/mL. Cell growth monitoring and biomass harvesting at different growth phases for antioxidant assays.

The cell density was observed daily for 24 days. The growth curve of each species was plotted by the total number of cell densities against cultivation time (days) to determine the growth phases. For the determination of the wet and dry biomass, enzymatic as well as the non-enzymatic antioxidant assays, the cells were harvested at the lag (I), log (II), early stationary (III), mid stationary (IV), and death (V) phases at day 1, 4, 8, 16, and 24, respectively. All results are presented as means and standard deviation ($n = 5$).

Determination of cell density

The growth of each culture was assessed by monitoring cell density daily for 24 days. Approximately 1 mL



of the microalgae liquid culture was taken using a sterile 10 mL syringe filter and was transferred into a 1.5 mL microcentrifuge tube. About 200 μL of the liquid culture was diluted with 800 μL of Lugol's solution. Ten μL of the diluted solution was transferred into an improved Neubauer hemocytometer cavity. The cell density was calculated following the method by Sahastrabudde (2016).

$$\text{Cell density (cells/mL)} = \frac{\text{Total cells number} \times \text{dilution factor}}{\text{Total squares number} \times \text{Square volume at 0.01 mm depth}}$$

Determination of wet and dry biomass

Microalgae cells were harvested by centrifuging (Allegra X-30R Centrifuge, Beckman Coulter, Inc., Germany) at 10,000 rpm and $24 \pm 2^\circ\text{C}$ for 10 min in 50 mL falcon tubes to get the fresh pellets. The pellets were washed off with distilled water three times to remove the dissolved salts in the medium. The pellets were weighed for wet biomass (g/L). Then, each pellet was further dried in an oven at $70 \pm 2^\circ\text{C}$ for 24 h until it obtained the persistent weight to give the dry biomass (g/L) (Kong et al. 2011).

Determination of enzymatic antioxidants

Superoxide dismutase (SOD) was extracted according to the method of Price et al. (1994) with some modifications. The fresh sample was homogenised with 1 mL of 100 mM potassium phosphate buffer (pH 7.0) using an ultrasonic bath (Fisherbrand™ Elmasonic S 60H, Fisher Scientific, Germany) for 10 min at 4°C . The homogenate was centrifuged (Microfuge 20R Centrifuge, Beckman Coulter, Inc., Germany) at 10,000 rpm and 4°C for 10 min. The reaction rate was measured at 550 nm every 30 s for 5 min at 25°C .

Catalase (CAT) was extracted according to the method of Claiborne (1985) with some alterations. The fresh sample was homogenised with 1 mL of 50 mM potassium phosphate buffer (pH 7.4). The CAT-specific activity was determined by measuring the decrease in the reaction rate at 240 nm and calculated using a $43.6 \text{ M}^{-1} \text{ cm}^{-1}$ extinction coefficient.

Ascorbate peroxidase (APX) was extracted according to the method of Sairam et al. (1997) with some alterations. The fresh sample was homogenised with 1 mL of 100 mM potassium phosphate buffer (pH 7.0) containing 1 mM L-ascorbic acid. The homogenate was centrifuged, and the reaction rate was measured at 290 nm every 30 s for 5 min at 25°C . The APX-specific activity was calculated using the $2.8 \text{ mM}^{-1} \text{ cm}^{-1}$ extinction coefficient.

Guaiacol peroxidase (GPX) was extracted using the method of Agrawal and Patwardhan (1993) with some modifications. The reaction rate was measured at 436 nm every 30 s for 3 min at 25°C , and the specific activity was calculated using the $26.6 \text{ mM}^{-1} \text{ cm}^{-1}$ extinction coefficient.

Glutathione reductase (GR) was extracted according to the method of Carlberg and Mannervik (1985) with some alterations. The reaction rate was measured at 415 nm every 30 s for 3 min at 25°C . The GR-specific activity was calculated using the $6.22 \text{ mM}^{-1} \text{ cm}^{-1}$ extinction coefficient.

Protein concentration

Protein concentration was estimated according to the method by Bradford (1976). Bradford's solution was prepared by dissolving 0.1 g of Coomassie Brilliant Blue G-250 into 50 mL of 95% (v/v) ethanol. Subsequently, 100 mL of 80% concentrated phosphoric acid was combined into the Coomassie Brilliant Blue G-250 mixture. The mixture was made up to 1 L using distilled water in a volumetric flask. This solution was filtered using the filter paper in a fume hood for appropriate ventilation. The solution was stored in the refrigerator in an amber borosilicate bottle. Protein concentration was determined by adding 150 μL of Bradford's solution and 50 μL of supernatant. The microplate was shaken and incubated at 25°C for 10 min in the microplate reader (Varioskan™ LUX, Thermo Fisher Scientific, Finland) before the absorbance at 595 nm was measured. A standard curve was prepared using Bovine Serum Albumin (BSA) at 0 to 100 $\mu\text{g/mL}$, and the amount of protein in the sample was calculated based on the standard curve prepared.



Determination of non-enzymatic antioxidants

Chlorophylls (Chls) and Carotenoids (CAR) were extracted according to the method of Torres et al. (2014). The fresh sample was homogenised with 1.5 mL of absolute methanol for 10 min at 4°C. The homogenate was centrifuged at 10,000 rpm and 4°C for 10 min. About 200 µL of supernatant was transferred into a flat bottom 96-well plate. The microplate was shaken for 10 s in the microplate reader (Varioskan™ LUX, Thermo Fisher Scientific, Finland). The Chls and CAR were measured at 470, 653, and 666 nm.

Ascorbic acid (AsA) content determination was adapted according to the procedure of Norhayati et al. (2016) with minor modifications. The absorbance of the mixture was measured at 760 nm. A standard curve was prepared using AsA at 0 to 5 µg/mL, and the amount of AsA in the sample was calculated based on the standard curve obtained.

α-Tocopherol (TOC) was assayed according to the method of Norhayati et al. (2016) with some modifications. Under dim light and on ice, the fresh sample was homogenised with 1.5 mL acetone at 4°C for 10 min. The mixture was extracted with 0.5 mL hexane. The homogenate was centrifuged at 10,000 rpm and 4°C for 10 min. After the centrifugation, the top layer was removed, and the hexane extraction was repeated twice. The absorbance of the reaction mixture was measured at 554 nm. A standard curve was prepared using standard TOC at 0 to 100 µg/mL, and the amount of TOC in the sample was calculated based on the standard curve.

Total glutathione was assayed according to the method of Janknegt et al. (2009). The fresh sample was homogenised with 1 mL of 50 mM 5-sulfosalicylic acid, 1 mM EDTA, and 0.15% L-ascorbic acid at 4°C for 10 min at 0–4°C. The homogenate was centrifuged at 10,000 rpm at 4°C for 10 min. For the total GSH, 10 µL of supernatant was transferred into a flat bottom 96-well plate. Then, 150 µL of reaction mixture consisting of 100 mM potassium phosphate buffer (pH 7.0), 100 mM Ethylene diamine tetra acetic acid disodium salt dihydrate (EDTA), 0.11 mM DTNB and 0.17 U/mL GR was added to start the reaction. Next, the microplate was left for 5 min for the conversion of GSSG to GSH, and then 50 µL of 0.2 mM β-NADPH was added. Finally, the reaction rate was measured immediately at 405 nm with an interval of every 30 seconds for 10 min at 25°C in the microplate reader. A standard curve was prepared using reduced GSH at 0 to 0.5 nmoles, and the amount of total GSH in the microalgal sample was calculated based on the standard curve.

Statistical analysis

Data were expressed as means and standard deviation (SD) of five replications. The normality tests were performed using skewness and kurtosis. One-way analysis of variance (ANOVA) was used to determine treatment mean differences. Multiple means comparison was determined by a Tukey's test at a 95% significance level. Correspondence Analysis (CA) was analysed using Paleontological Statistics Software Package (PAST) version 4.03.

Results and discussion

Figure 1 shows images of *C. vulgaris*, *I. galbana*, and *T. chui* under a compound light microscope at 400× magnification and Scanning Electron Microscope (SEM), taken from inoculum cultures during the early stationary phase on day 8. It was observed that *T. chui*'s cells are bigger than those of *C. vulgaris* and *I. galbana*. *T. Chui* cells have an oval shape and can grow up to 14 µm in length and 10 µm in breadth (Kokkali et al. 2020). *C. vulgaris* exhibits a spherical shape with a diameter of 4 µm, consistent with the findings of Chioccioli et al. (2014). The cell size of *I. galbana* varies from 5 to 6 µm in length and 2 to 4 µm in width. Both *I. galbana* and *T. chui* are flagellated microalgae; however, the flagella were absent in these samples, likely due to the drying process.

Microalgae growth phases and their biomass

The growth curve pattern exhibited in this study can be divided into four primary phases: lag, log, stationary, and death, which are comparable to those reported by Kasan et al. (2020) in *Chlorella* sp., *Nannochlo-*



ropsis sp., and *Desmodesmus* sp. Consequently, the growth curve of *C. vulgaris*, *I. galbana*, and *T. chui* in this study was defined as follows: lag (I), log (II), early stationary (III), mid-stationary (IV), and death (V) phases occurring on days 1, 4, 8, 16, and 24, respectively (Figure 2). Based on these findings, samples were harvested on these selected days for antioxidant determination.

Wet and dry biomass measurements of *C. vulgaris*, *I. galbana*, and *T. chui* were conducted throughout the growth phases, as illustrated in Figure 3. Measuring both wet and dry biomass is crucial because each provides distinct insights into the studied microalgae species. Wet biomass reflects the fresh weight, making it useful for short-term physiological studies or when analyzing processes related to water content. However, since the water content in wet biomass can fluctuate due to environmental factors, it is not a consistent measure of the actual organic material (Huang et al. 2019). In contrast, dry biomass represents the mass after removing all water, typically by drying the sample at a controlled temperature. This method offers a more stable and accurate measure of the actual organic matter, including essential elements like carbon, nitrogen, and other nutrients that contribute to the structure of the species. As a result, dry biomass is often considered a more reliable metric for assessing productivity or health over time or across different environments, as it excludes the variability caused by water content (Godbey 2021).

In this study, the wet and dry biomass increased significantly from the lag phase to the early stationary phase in all three species. A plateau pattern was observed from the early stationary phase onwards in *C. vulgaris* and *T. chui*. However, in *I. galbana*, both the wet and dry biomass were higher during the mid-stationary and death phases. The differences in biomass patterns observed among the three species during their growth phases can be explained by various biological and environmental factors that impact their growth dynamics, metabolism, and biomass accumulation. Both *C. vulgaris* and *T. chui* follow a typical growth curve, where biomass reaches a plateau during the stationary phase. This phase occurs as growth slows due to limiting factors like nutrient depletion, accumulation of metabolic waste, or reduced light availability (Mata et al. 2010). At this stage, cell division decreases or halts, resulting in a stabilization of biomass. These microalgae likely conserve energy and resources to survive in suboptimal conditions. The plateau in both wet and dry biomass suggests that while the cells remain alive, they are no longer growing

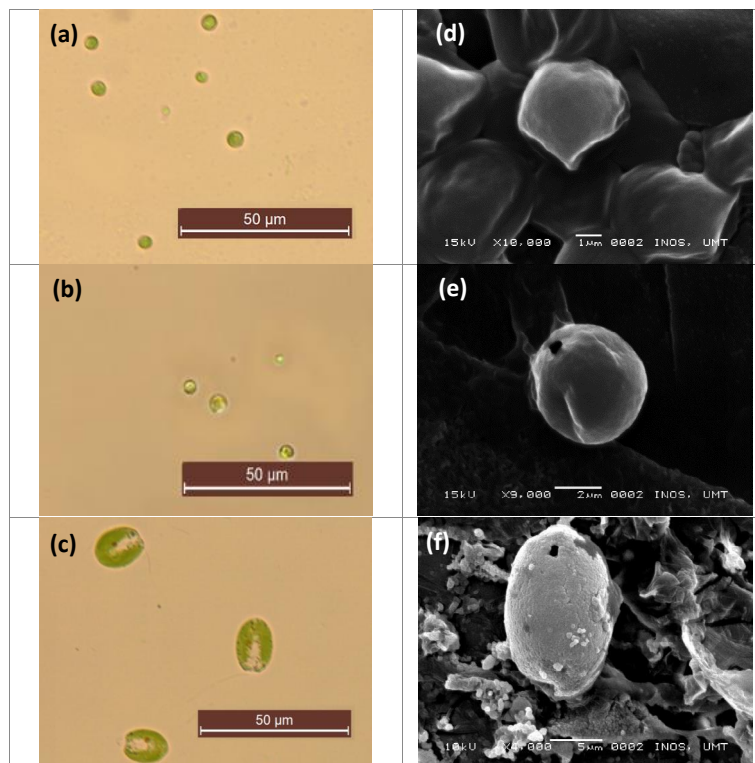


Fig. 1 Compound light microscope images (400× magnification) of microalgae (a) *C. vulgaris*, (b) *I. galbana*, (c) *T. chui*, and scanning electron microscope (SEM) images of microalgae (d) *C. vulgaris*, (e) *I. galbana*, (f) *T. chui* during early stationary phase, with lines indicating the microalgae size (μm).



or accumulating additional organic matter. *I. galbana* is well-known for its high lipid and carbohydrate accumulation, especially under stress conditions like nutrient limitation. The increase in biomass could be due to this accumulation of storage molecules, contributing to a higher dry weight even as cell division slows. Additionally, *I. galbana* may adapt to stationary phase conditions by enlarging individual cell size as a survival strategy, which would lead to an increase in wet biomass. Cells likely swell as they store nutrients such as lipids and carbohydrates in preparation for unfavourable conditions (Hu et al. 2008). This allows *I. galbana* to continue metabolizing and accumulating biomass longer than *C. vulgaris* and *T. chui* during the stationary phase, resulting in sustained biomass accumulation even into the death phase.

The lag phase of *C. vulgaris*, *I. galbana*, and *T. chui* cells took only one full day to adapt to their new environment before they grew more rapidly and increased their biomass. Similarly, Kasan et al. (2020) observed a one-day lag phase in *Chlorella* sp., *Nannochloropsis* sp., and *Desmodesmus* sp. The lag phase commonly occurs as microalgae adapt to new cultivation conditions, such as changes in medium composition, pH, and light (Belaïdi et al. 2020). During this phase, cell growth is slow, resulting in low wet and dry biomass. However, this slow growth may stimulate the production of enzymes and metabolites necessary for cell division. It is also suggested that microalgae might experience photoinhibition during low cell density due to persistent light penetration and a lack of self-shading (Kasan et al. 2020).

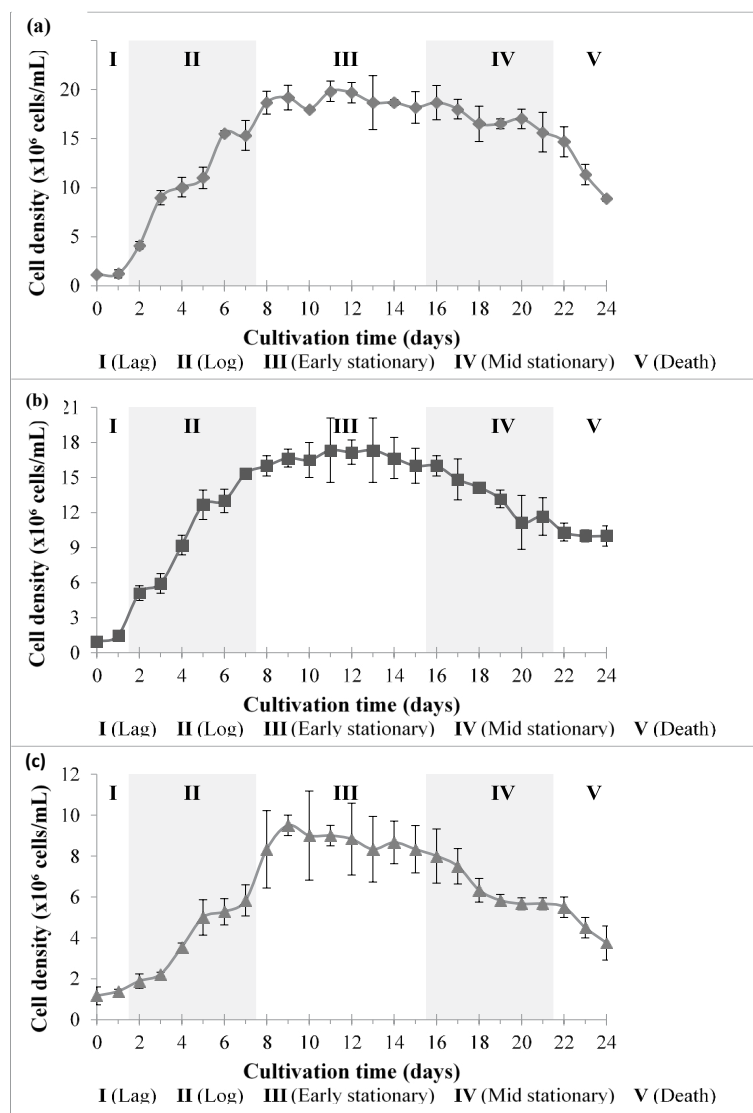


Fig. 2 Growth curve of (a) *C. vulgaris*, (b) *I. galbana*, and (c) *T. chui* throughout 24 days of cultivation. Capital Roman numerals I, II, III, IV, and V correspondingly represent lag, log, early stationary, mid stationary, and death phase, respectively. Data presented are means \pm SD



All three microalgae species exhibited rapid cell growth from day 2 to 7, marking the log phase, where both wet and dry biomass increased significantly. This might be due to nutrient availability in the medium. During the initial stages of the culture, the medium is rich in essential nutrients such as nitrogen, phosphorus, and trace elements. These nutrients can activate the cell's metabolic activities, thus signalling cellular processes like protein synthesis, photosynthesis, and cell division. As a result, microalgae cells rapidly absorb these nutrients, leading to an exponential increase in biomass (both wet and dry) during the log phase. In addition, at this phase, factors such as temperature, pH, and CO₂ availability are often maintained within optimal ranges. These conditions ensure that the cells are not experiencing stress, which would otherwise slow down growth. Instead, they can focus on replication and biomass accumulation (Belaïdi et al. 2020).

The stationary phases for *C. vulgaris*, *I. galbana*, and *T. chui* were observed from day 8 to day 22, divided into early stationary (day 8) and mid-stationary (day 16) phases. In the early stationary phase (day 8), growth has significantly slowed but is still somewhat active as cells continue metabolizing remaining nutrients. By the mid-stationary phase (day 16), growth has nearly ceased, and the cultures are stable, with limited cell division and biomass production as the cells shift focus to maintaining cellular function and possibly preparing for stressful conditions (Jaishankar and Srivastava 2017). As microalgae enter the stationary phase, essential nutrients like nitrogen and phosphorus become depleted, slowing growth due to limited resources for cell division and biomass accumulation. Increased cell density also limits light, reducing photosynthetic efficiency, while the accumulation of metabolic byproducts further inhibits growth by creating stressful conditions. During this phase, microalgae often shift their metabolism toward producing secondary metabolites like lipids and antioxidants, which are valuable for stress resistance rather than biomass production (Ramlee et al. 2021).

During the death phase, *C. vulgaris*, *I. galbana*, and *T. chui* showed a slight decline in cell density from day 22 onwards, as cells could not sustain growth. In this phase, the number of dead cells exceeds that of living cells. The reduction in cell density during this final phase is due to nutrient starvation and other limiting factors such as pH changes, overheating, accumulation of toxic by-products, and contamination (Belaïdi et al. 2020).

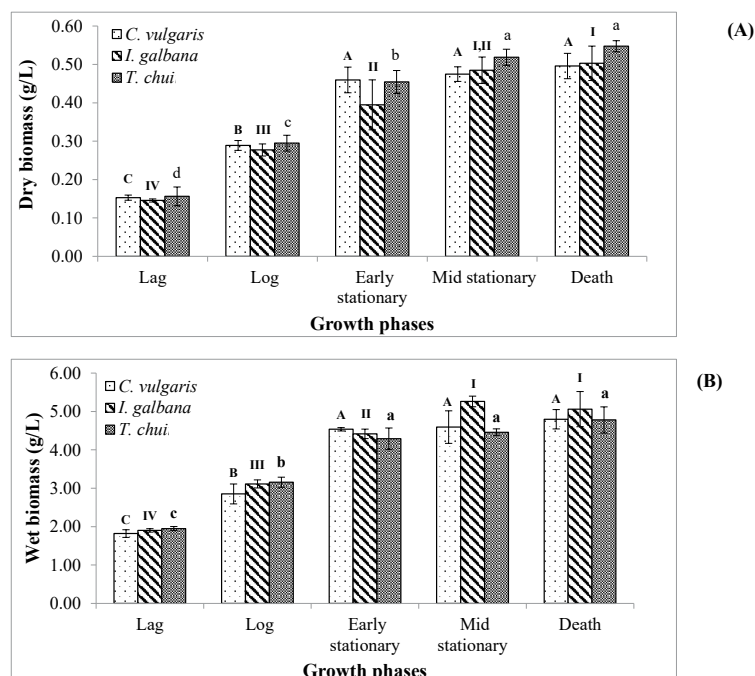


Fig. 3 Dry (a) and wet biomass (b) of *C. vulgaris*, *I. galbana*, and *T. chui* throughout growth phases. Data presented are means \pm sd. Capital letters (*C. vulgaris*), roman numerals (*I. galbana*) and small letters (*T. chui*) above the error bars represent significant differences throughout growth phases in individual species at $p < 0.05$.



Microalgal enzymatic antioxidants at different growth phases

Superoxide dismutase (SOD) activities

SOD activity in *C. vulgaris* slowly increased and maximum at the early stationary phase (0.37 ± 0.03 U/mg protein), followed by a steep drop from the mid-stationary-to-death phase. Accumulation of SOD activities is species-specific at certain growth phases where *S. armatus* has the highest SOD activity at the log phase, whilst *S. obliquus* at the lag phase (Pokora et al. 2003). These findings were in line with the variations of SOD activities in *C. vulgaris*, *I. galbana*, and *T. chui* throughout the growth phases (Figure 4A). These activities were higher than previous results reported in four different strains of *C. vulgaris* which ranged from 0.03 to 0.09 U/mg protein (Chatzikonstantinou et al. 2017). In *I. galbana*, SOD activity was highest at the initial growth phase, which is similar to reported in *T. gracilis* (Sigaud-Kutner et al. 2002) and *C. vulgaris* (Sun et al. 2014). Lower SOD activity in *I. galbana* ranging from 0.099 ± 0.003 to 0.199 ± 0.001 U/mg protein compared to the results reported by Jin et al. (2020) in the same species of 0.2 to 1.0 U/mg protein. In *T. chui*, the maximum SOD activity was obtained during the log phase and reduced onwards.

The increment of SOD activity in *C. vulgaris* and *I. galbana* during the stationary phase as a first line of cellular defence mechanism toward ROS accumulation, suggests that the microalgal cellular tolerance toward oxidative stress was induced by scavenging excess of $O_2^{\cdot-}$ generation to H_2O_2 and O_2 in the chloroplast, mitochondria, cytosol, and extracellular space of the microalgae (Zhang et al. 2020). The obtained results suggest that both microalgae are responding to heightened oxidative stress brought on by nutrient limitation and increased ROS accumulation during this period of reduced growth. The observed activities might also be influenced by the limitation of CO_2 fixation when the nutrients particularly nitrogen in the medium start to reduce, which leads to more electron leakage to O_2 molecules and initiates the ROS generation, especially $O_2^{\cdot-}$ (Hasanuzzaman et al. 2020). After this point, as the culture progresses into the mid-stationary and death phases, cell viability declines, and metabolic activity slows down. This leads to a reduction in both ROS production and the need for SOD-mediated protection, which explains the sharp drop in SOD activity.

Higher SOD activity in *I. galbana* during the lag phase might be attributed to photoprotection by SOD against light sources. This is because chlorophyll synthesis is limited by photoinhibition, which occurs due to a lack of self-shading when the light source persistently penetrates individual cells during low cell density. In the lag phase, cells adjust to new environmental conditions and initiate metabolic processes, which can lead to moderate levels of ROS. The increased SOD activity in this phase would indicate that the cells are preparing for elevated oxidative stress as metabolism ramps up. Conversely, the increase in SOD activity in *T. chui* during the log phase is likely associated with intense photosynthetic activity causing chloroplast-localized stress (Sigaud-Kutner et al. 2002). Thus, higher ROS generation is a byproduct of active metabolism and photosynthesis. The elevated SOD activity during the log phase is crucial for detoxifying the superoxide radicals produced under these high-energy conditions, ensuring that cellular functions are protected from oxidative damage during this period of exponential growth. The significant decline of SOD in *C. vulgaris* during the death phase indicates excessive accumulation of $O_2^{\cdot-}$, surpassing the capability of SOD activity. This imbalance between dismutation activities and $O_2^{\cdot-}$ production results in significant cellular damage as microalgae cells enter the depletion phase (Ugya et al. 2020).

Catalase (CAT) activities

CAT is crucial in the SOD-CAT system, breaking down H_2O_2 into harmless O_2 and H_2O (Zhang et al. 2020). Figure 4B depicts the CAT activities in the three studied microalgae species throughout the growth phases. In *C. vulgaris*, CAT activity fluctuated from the lag to stationary phases and decreased during the death phase. The CAT activity observed in this study was lower compared to those reported by Ismaiel et al. (2016) in *A. platensis*. In *I. galbana*, CAT was significantly induced during the log and stationary phases compared to other phases, consistent with findings in *C. vulgaris* (Sun et al. 2014) and *M. aeruginosa* (Giannuzzi et al. 2016). *T. chui* exhibited the highest CAT activities in the log phase, with lower activities during other growth phases.

CAT is an antioxidant enzyme that acts as a cellular defence against H_2O_2 , a precursor of the highly



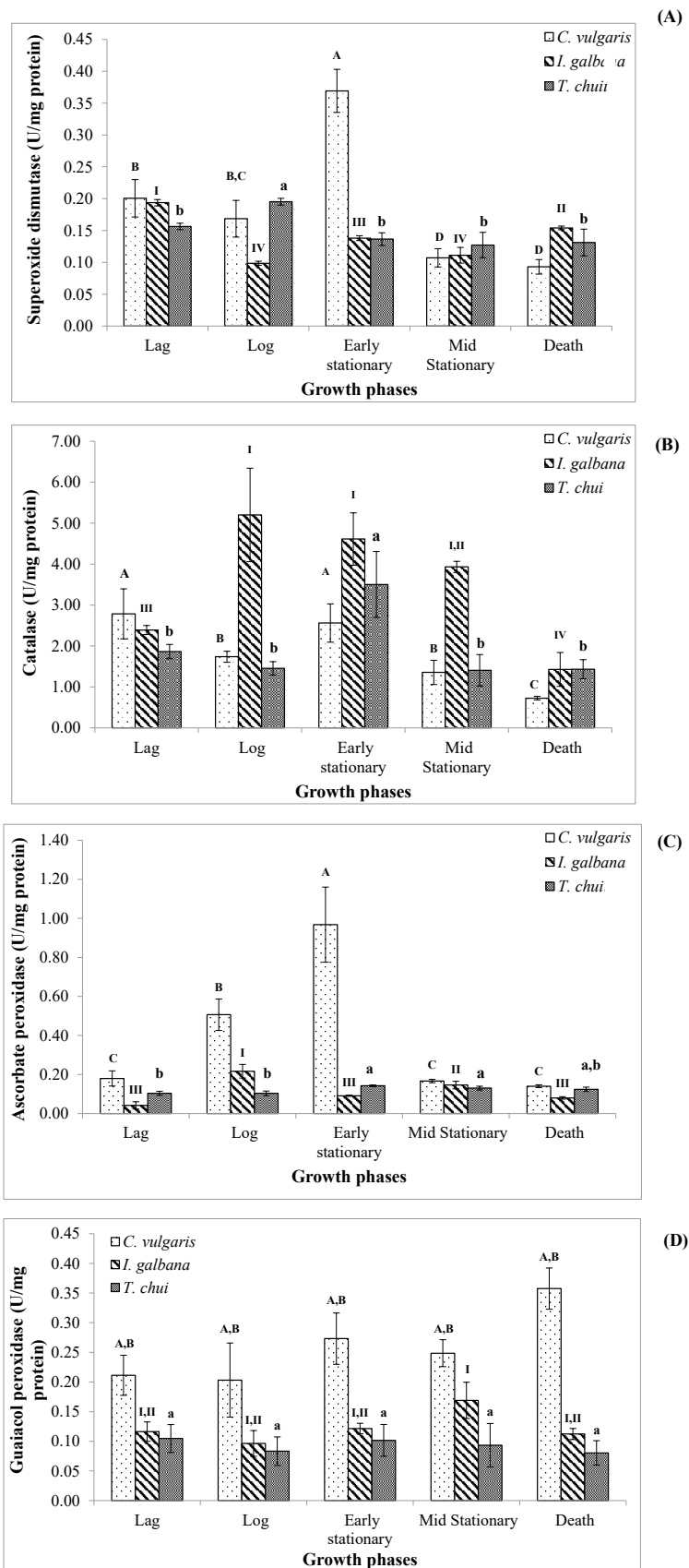


Fig. 4 Superoxide dismutase (A), Catalase (B), Ascorbate peroxidase (C), Guaiacol peroxidase (D) and Glutathione reductase (E) activities of *C. vulgaris*, *I. galbana*, and *T. chui* throughout growth phases. Data presented are means ± SD. Capital letters (*C. vulgaris*), Roman numerals (*I. galbana*) and small letters (*T. chui*) above the error bars represent significant differences throughout growth phases in individual species at P<0.05.



reactive and dangerous OH^\cdot free radical and helps oxidize H_2O_2 molecules into H_2O and O_2 . The decline of CAT activity in *C. vulgaris* from the lag to log phase might be due to the emergence of other effective H_2O_2 quenchers, particularly peroxidases (Ansari et al. 2021). The increase in CAT activity in *C. vulgaris*, *I. galbana*, and *T. chui* at the early stationary phase is primarily linked to the need for detoxification of the overproduction of H_2O_2 . As the microalgae transition to this phase, nutrient availability decreases, causing metabolic shifts that elevate oxidative stress. Specifically, the lack of essential nutrients, combined with the accumulation of metabolic by-products, triggers the production of ROS, including H_2O_2 . Thus, CAT activity rises in response to the elevated H_2O_2 levels to prevent cellular damage, ensuring cell survival under stress conditions (Javier et al. 2018).

Additionally, Sigaud-Kutner et al. (2002) suggested that nitrogen deprivation in microalgae can critically promote oxidative damage during the stationary phase. The further reduction of CAT in *C. vulgaris*, *I. galbana*, and *T. chui* from early stationary onwards suggests that the microalgae cells had reached oxidative saturation, where the amount of H_2O_2 produced surpassed the antioxidative capacity during unfavourable growth conditions, leading to a decrease in CAT enzyme synthesis. The inactivation of CAT by ROS can affect membrane lipids via lipid peroxidation, ultimately leading to cell death (Cheng et al. 2016).

In this current study, SOD activity was highest in *C. vulgaris* during the early stationary phase (Figure 4A), while CAT activity was not elevated to the same extent (Figure 4B). This might be related to the differential regulation of antioxidant enzymes. Although SOD and CAT often work in tandem, their regulation can be independent based on the nature and intensity of oxidative stress. In the early stationary phase, *C. vulgaris* might prioritize SOD production to manage $\text{O}_2^{\cdot-}$, while the subsequent detoxification of H_2O_2 by CAT may depend on other antioxidant systems like peroxidases; APX (Figure 4C) and GPX (Figure 4D) or glutathione-based enzymes (Ansari et al. 2021). Results also revealed that CAT activities were significantly higher in *I. galbana* especially in log, early and mid-stationary phases compared to other species. This might be related to different microalgae species possessing varying metabolic strategies to cope with oxidative stress. *I. galbana* may prioritize H_2O_2 detoxification over $\text{O}_2^{\cdot-}$ neutralization due to differences in the cellular processes that generate these ROS, necessitating a stronger CAT response to mitigate the toxic effects.

Peroxidase activities

Ascorbate peroxidase (APX) in *C. vulgaris* rose gradually until it reached maximum activity during the early stationary phase, following a steep decline after that. Interestingly, *I. galbana* exhibited a fluctuating pattern of APX activity, peaking during the log phase. In contrast, APX in *T. chui* increased significantly and maintained consistent activity from the early stationary phase onwards, with a slight drop during the death phase (Figure 4C). Guaiacol peroxidase (GPX), another enzyme that detoxifies H_2O_2 , showed a slight elevation pattern in *C. vulgaris* throughout the growth cycle, with the highest activity observed in the death phase. In *I. galbana*, GPX activity increased slowly from the early to mid-stationary phase and then de-

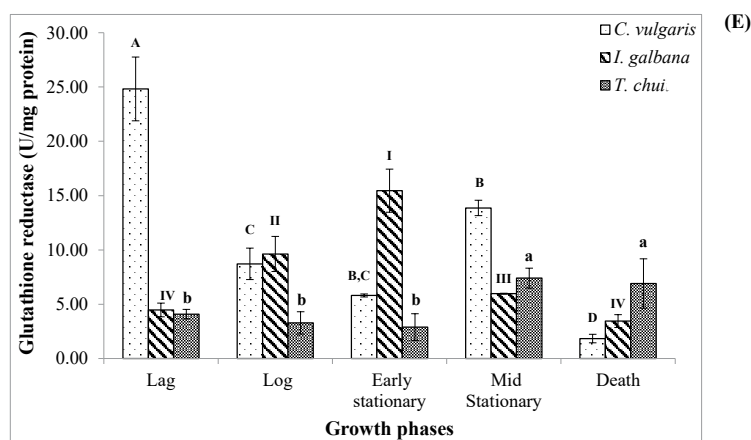


Fig. 4 Continued



clined during the death phase. In *T. chui*, different growth phases did not significantly affect GPX activities (Figure 3D). These results align with findings reported by Sun et al. (2014) in *C. vulgaris* cultures. The induction of peroxidase enzymes is associated with their role in scavenging H_2O_2 , the most stable ROS (Giannuzzi et al. 2016). Although both APX and GPX are heme-containing enzymes, they differ in electron donor preference: AsA is an electron donor for APX, while guaiacol acts as an aromatic electron donor for GPX (Sharma et al. 2012; Rezayian et al. 2019). Among H_2O_2 -scavenging enzymes, APX has been reported to be more effective than CAT or GPX due to its higher affinity for H_2O_2 (Roy et al. 2021). The elevation of APX activities in *C. vulgaris* during the early stationary phase and in *I. galbana* during the log phase can be attributed to the enzyme's role in scavenging H_2O_2 to mitigate oxidative stress in cell compartments such as chloroplasts, cytosol, mitochondria, and peroxisomes (Roy et al. 2021).

During the death phase, decreased APX activity in *C. vulgaris* and *I. galbana* might be due to the enzyme's inability to protect cells from oxidative damage when excessive ROS is produced or due to a drop in enzyme synthesis caused by pigment deficiency and degradation of thylakoid membranes (Cheng et al. 2016; Javier et al. 2018). *T. chui* exhibited higher APX activity in the last three phases, likely due to oxidative protection needs arising from essential nutrient deprivation, such as nitrogen.

Initially, the GPX activities of *C. vulgaris* and *I. galbana* may not have functioned effectively due to low levels of ROS production in the cells. However, as the growth phases progressed, GPX activities in these species increased, likely protecting against increased ROS generation. GPX activity was not significantly promoted in *T. chui*, suggesting that other antioxidants, such as CAT and APX, play a predominant role in scavenging bulk H_2O_2 . Therefore, it is suggested that GPX may be involved in detoxifying H_2O_2 residues.

Glutathione reductase (GR) activities

Figure 4E shows that *C. vulgaris* has the highest GR activity at the lag phase and fluctuates after that. In contrast, a study by Chen et al. (2020) revealed that *C. vulgaris* has higher GR activity during the early stationary phase. GR activities in *I. galbana* significantly increased at the lag to early stationary phase, followed by a drastic decline at the two last phases. Meanwhile, a stagnant GR in *T. chui* from the beginning to the early stationary phase was observed before markedly going up at the mid-stationary phase and maintained higher until the death phase. The increase of GR activity in *C. vulgaris* during the lag phase and in *I. galbana* during the early stationary phase might indicate the tolerance of microalgae toward oxidative metabolism by the glutathione metabolic pathway (Cheng et al. 2016). GR will sustain a high cellular GSH/GSSG ratio in cell cytoplasm through the interconversion of reduced GSH to GSSG using NADPH (Singh and Patidar 2018). In addition, the GR induction was observed in *I. galbana* during the early stationary phase, suggesting its function to scavenge H_2O_2 produced via the Mehler reaction in the chloroplast. The rising of GR in *T. chui* during the mid-stationary to death phases is possibly related to the collaborative relation with APX, as reported in *P. tricornutum*. Both GR and APX participated in the ascorbate-glutathione (AsA-GSH) pathway, also known as the Halliwell-Asada pathway, where GSH and NADPH are utilised to regenerate AsA (Sharma et al. 2012).

Microalgal non-enzymatic antioxidants at different growth phases

Chlorophylls and carotenoid contents

Chls are important in photosynthesis to absorb light energy and transmit the excited electrons to the reaction, which takes part in light reactions and the Calvin cycle. Chl a is the most abundant pigment in converting light energy to chemical energy, whereas Chl b acts as an accessory pigment to aid in absorbing light energy and passing it to Chl a (Ren et al. 2019). In this current study, Chl a in *C. vulgaris* gradually increased from the lag phase, reaching a maximum value in the mid-stationary phase (1.77 ± 0.04 mg/gfw), before sharply dropping in the death phase. A similar trend was observed in *I. galbana*. This ascending pattern of Chl a in both *C. vulgaris* and *I. galbana* from lag to stationary phases is consistent with previous studies on *C. vulgaris* (Sun et al. 2014), *Chlorella* sp., and *N. oculata* (Paes et al. 2016). For *T. chui*, the increment of Chl a was notable during the log phase, followed by a reduction after that. The trends in Chl b content were similar to those of Chl a for *C. vulgaris*, *I. galbana*, and *T. chui*, though generally, these three



species accumulated lower Chl b content compared to Chl a (Table 1).

Nutrient depletion, particularly essential nitrogen, significantly affects Chls a and b levels because these pigments are nitrogen-rich compounds. When microalgae attain a stationary phase, the essential nutrients start to deplete, and the metabolic toxins begin to elevate (Bauer et al. 2017). The emergence of Chls in *C. vulgaris* and *I. galbana* at the stationary phase suggests a photoprotective role of these pigments by increasing the dissipation of excitation energy from the reaction centres during nutrient starvation. The subsequent rise in Chls during the stationary growth phase also acts as photo acclimation toward light competition, as light is one of the limiting factors that alter the photosynthetic pigments as reported in *T. gracilis* (Sigaud-Kutner et al. 2002). The decline in Chls a and b content in three microalga species during the death phase might be due to cellular aging. Additionally, food limitations contribute to the reduction of chlorophylls, as nutrient insufficiency diminishes chlorophyll levels, accessory pigments, and light collection efficiency over time (Bauer et al. 2017).

CAR complements Chl a as accessory pigments, aiding in light absorption and energy dissipation to Chl a in photosynthesis, and also plays a role in stabilising chloroplast membranes and providing photoprotection (Sun et al. 2014; Ren et al. 2019). The CAR levels in *C. vulgaris* and *I. galbana* increased from the lag to the stationary phase, followed by a decline in the death phase. This rising pattern was also observed in previous studies on *C. vulgaris* (Sun et al. 2014), *C. kessleri* (Bauer et al. 2017), and *I. galbana* (Rahman et al. 2020). In contrast, CAR in *T. chui* was highest during the log phase (Table 1), consistent with findings in *T. suecica* (Rahman et al. 2020). The efficiency of CAR content in *C. vulgaris* and *I. galbana* in scavenging $^1\text{O}_2$ and quenching ^3Chl during the stationary growth phase is largely influenced by the presence of β -carotene, violaxanthin, neoxanthin, lutein, and zeaxanthin (Rahman et al. 2020). The high production of CAR in *T. chui* during the log phase indicates significant levels of lutein and β -carotene, followed by neoxanthin and zeaxanthin. The decline in CAR content observed in *C. vulgaris*, *I. galbana*, and *T. chui* during the death phase may be due to cell density reduction, nutrient limitations, and thylakoid membrane deterioration, leading to decreased photosynthetic rates and CO_2 assimilation (Javier et al. 2018; Rahman et al. 2020).

Ascorbic acid (AsA) content

AsA is vital in quenching ROS and functioning as an electron donor for APX-mediated H_2O_2 detoxification (Rezayian et al. 2019). It was demonstrated that AsA content in *C. vulgaris* went up at the mid-stationary phase and was inhibited at the death phase. In *I. galbana*, AsA content was initially enhanced before being further reduced at the death phase. Contrarily, AsA content in *T. chui* was almost maintained throughout the cultivation phases and slightly dropped at the log phase (Figure 5A). Interestingly, the AsA contents in this study were in the range as reported in other microalgae species like *Nannochloropsis* sp. (0.6 mg/g FW), *Chlorella* sp. (1.5 mg/g FW), and *Chaetoceros* sp. (1.88 mg/g FW), as well as higher than some fruits

Table 1 The chlorophyll a, chlorophyll b and carotenoids of *Chlorella vulgaris*, *Isochrysis galbana* and *Tetraselmis chui* at different growth phases. Data presented are means \pm SD. Small letters above the error bars represent significant differences at $P < 0.05$

Species	Growth phase	Pigments		
		Chlorophyll a (mg/g. fwt)	Chlorophyll b (mg/g.fwt)	Carotenoids (mg/g.fwt)
<i>Chlorella vulgaris</i> (UMT-M1)	Lag	0.56 \pm 0.09 ^d	0.29 \pm 0.05 ^{c,d}	0.07 \pm 0.001 ^d
	Log	0.81 \pm 0.06 ^c	0.41 \pm 0.06 ^c	0.12 \pm 0.02 ^c
	Early stationary	1.34 \pm 0.04 ^b	0.71 \pm 0.02 ^b	0.26 \pm 0.08 ^b
	Mid Stationary	1.77 \pm 0.04 ^a	0.91 \pm 0.03 ^a	0.39 \pm 0.05 ^a
	Death	0.29 \pm 0.01 ^e	0.16 \pm 0.01 ^d	0.15 \pm 0.01 ^c
<i>Isochrysis galbana</i> (SWC002)	Lag	0.13 \pm 0.04 ^c	0.08 \pm 0.001 ^c	0.12 \pm 0.02 ^d
	Log	0.67 \pm 0.01 ^b	0.27 \pm 0.001 ^b	0.17 \pm 0.04 ^{b,c}
	Early stationary	0.74 \pm 0.05 ^b	0.32 \pm 0.009 ^{a,b}	0.18 \pm 0.02 ^b
	Mid Stationary	0.90 \pm 0.02 ^a	0.34 \pm 0.005 ^a	0.44 \pm 0.04 ^a
	Death	0.21 \pm 0.05 ^c	0.07 \pm 0.007 ^c	0.13 \pm 0.09 ^c
<i>Tetraselmis chui</i> (SWC001)	Lag	0.24 \pm 0.06 ^b	0.29 \pm 0.03 ^c	0.02 \pm 0.01 ^d
	Log	0.60 \pm 0.04 ^a	0.69 \pm 0.05 ^a	0.19 \pm 0.05 ^a
	Early stationary	0.58 \pm 0.03 ^a	0.51 \pm 0.09 ^{a,b}	0.15 \pm 0.09 ^b
	Mid Stationary	0.35 \pm 0.07 ^b	0.33 \pm 0.02 ^{b,c}	0.13 \pm 0.01 ^b
	Death	0.20 \pm 0.01 ^b	0.16 \pm 0.01 ^c	0.09 \pm 0.01 ^c



such as strawberries (0.54 mg/g FW), kiwis (0.52 mg/g FW), and lemons (0.42 mg/g FW) (Del Mondo et al. 2020). The higher AsA content in the studied microalgae, compared to the above-mentioned fruits, can be explained by several factors. Microalgae are exposed to fluctuating light, temperature, and nutrient conditions at different growth phases, thus inducing oxidative stress, prompting them to synthesize high levels of AsA as a protective mechanism. As efficient photosynthetic organisms, microalgae generate ROS during photosynthesis, and elevated AsA levels help neutralize ROS, preserving cellular health. In contrast, fruits grown in natural conditions may have limited AsA synthesis due to environmental factors. Differences in metabolic pathways also lead microalgae to prioritize antioxidant production under stress, further boosting AsA levels compared to terrestrial plants (Siddhath et al. 2024).

Induced AsA in all 3 species, particularly at the stationary phases are related to cell protection by directly scavenging the elevated level of $O_2^{\cdot-}$, $HO_2^{\cdot-}$, and OH^{\cdot} radicals, hence inhibiting photoinhibition of PSI. It also suggests the high function and capacity of AsA to donate electrons in both enzymatic reactions like

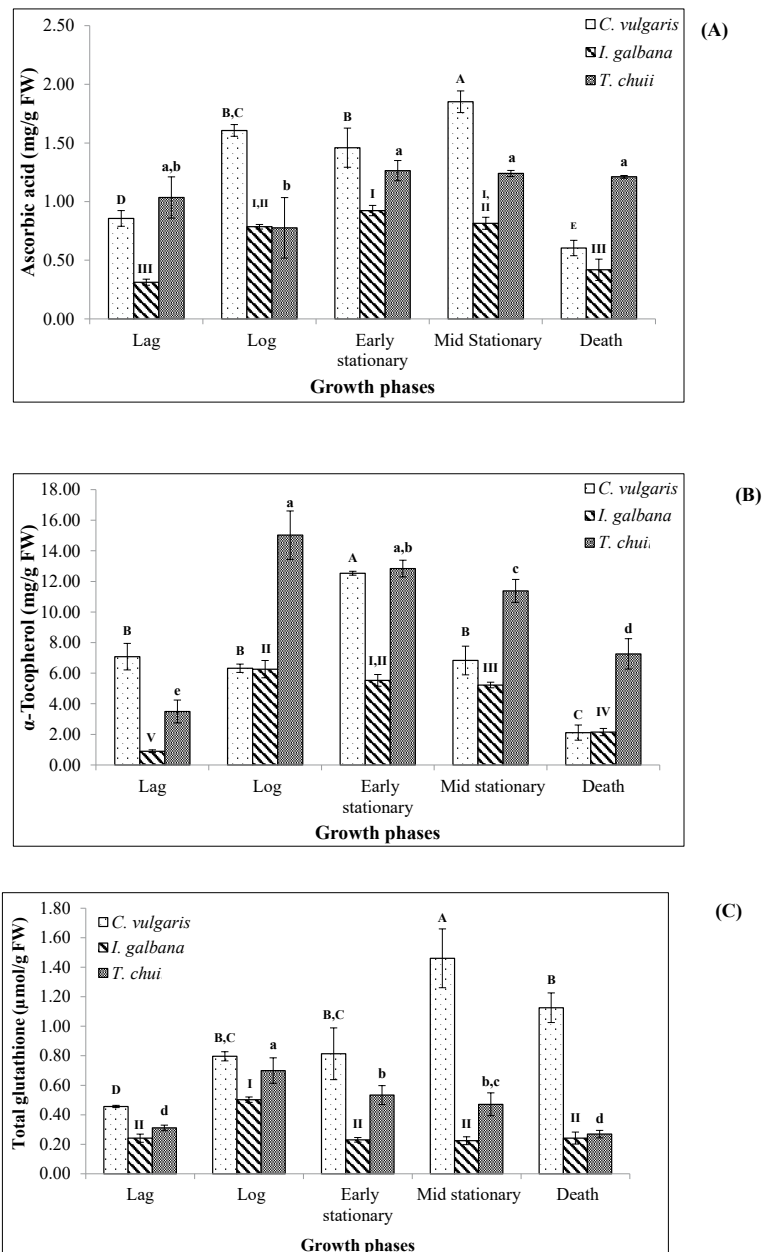


Fig. 5 Ascorbic acid (A), α -tocopherol (B) and total glutathione (C) of *C. vulgaris*, *I. galbana*, and *T. chui* throughout growth phases. Data presented are means \pm SD. Capital letters (*C. vulgaris*), Roman numerals (*I. galbana*) and small letters (*T. chui*) above the error bars represent significant differences throughout growth phases in individual species.



APX, and non-enzymatic pathways to regenerate TOC and GSH (Roy et al. 2021). Rapid depletion of AsA in the death phase described that reduction of AsA production is correlated with the physiological response to the depletion of inorganic macronutrients like nitrate (Del Mondo et al. 2020).

α -Tocopherol (TOC) content

TOC content in *C. vulgaris* was highest in the early stationary phase and gradually decreased after that. In contrast, TOC in *I. galbana* increased from lag to log phase, maintained at the stationary phase, and slightly decreased at the death phase. Meanwhile, TOC in *T. chui* drastically increased at the log phase and slowly reduced after that (Figure 5B). Interestingly, higher TOC was detected in this study, ranging from 6.27 ± 0.57 to 15.02 ± 1.58 mg/g FW compared to results in *C. sorokiniana* (0.66 ± 0.02 μ g/g FW) and *S. acuminatus* (0.08 ± 0.01 μ g/g FW) (Hamed et al. 2017).

In this study, the rising contents of TOC during log and early stationary phases indicate their role as a free radical chain-breaking antioxidant toward oxidative stress by detoxifying $^1\text{O}_2$, $\cdot\text{OH}$, and lipid peroxy radicals. The results were consistent with *E. gracilis* where the elevation of ROS production in the chloro-

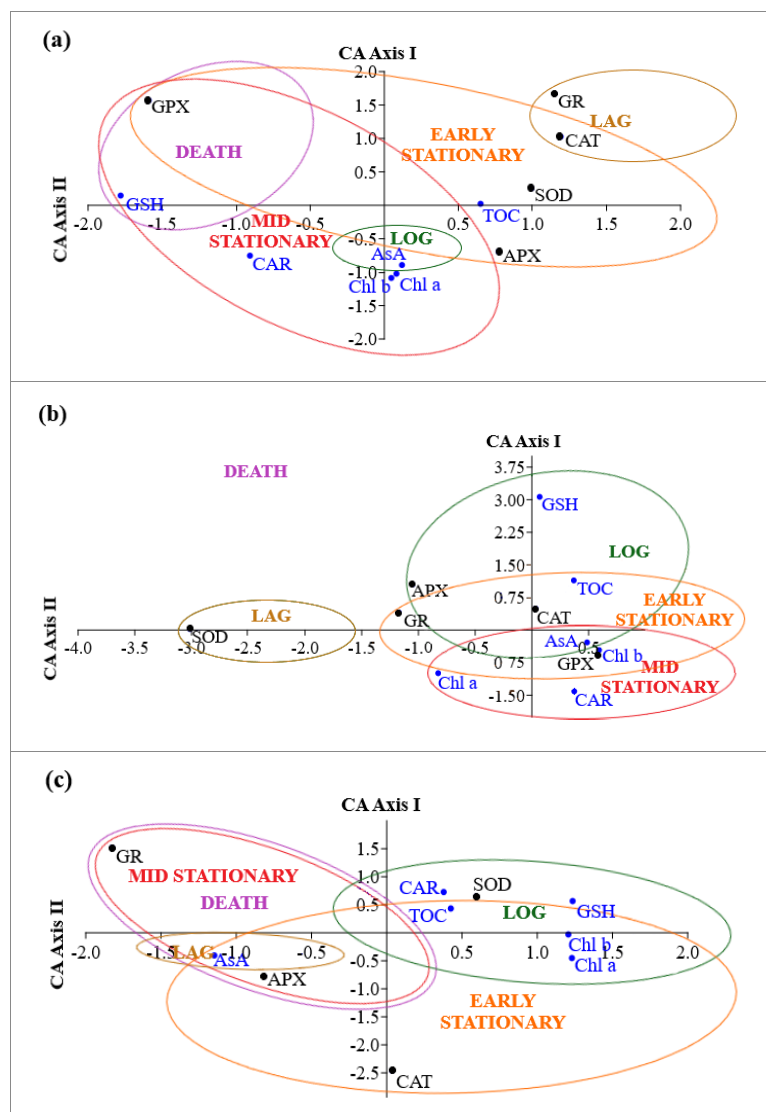


Fig. 6 Correspondence analysis (CA) on antioxidative responses distribution of microalgae (a) *C. vulgaris*, (b) *I. galbana*, and (c) *T. chui* at different growth phases. Enzymatic antioxidants (SOD, superoxide dismutase; CAT, catalase; APX, ascorbate peroxidase; GPX, guaiacol peroxidase; GR, glutathione reductase) are in black colours and non-enzymatic antioxidants (Chls, chlorophylls; CAR, carotenoids; AsA, ascorbic acid; TOC, α -tocopherol; GSH, total glutathione) are in blue colours.



plasts and mitochondria might enhance the production of TOC (Häubner et al. 2014). In addition, increased TOC suggests its function to break the lipid peroxidation reaction and protect unsaturated fatty acids from oxidation (Rezayian et al. 2019). A drop in TOC content during mid-stationary and death phases might be due to the cell density reduction, essential nutrients limitation, and thylakoid membrane deterioration, resulting in the descending of this lipid-soluble antioxidant (Javier et al. 2018; Rahman et al. 2020).

Total glutathione (GSH) content

In *C. vulgaris*, an increasing pattern of total GSH was detected from the lag to the mid-stationary phase and slowly dropped at the end of the growth. Total GSH in *I. galbana* and *T. chui* accumulated at the log phase and further declined throughout the growing periods (Figure 5C). Among non-enzyme antioxidants, GSH is the most abundant of low molecular weight non-protein thiol which is functionally important in enzymatic and non-enzymatic mechanisms. In this study, a significant increase in the GSH concentration at the mid-stationary phase might related to the adaptive responses of *C. vulgaris*, which acts as the potential scavenger of the most dangerous $\bullet\text{OH}$ radicals, as well as non-radicals of H_2O_2 and $^1\text{O}_2$ (Rezayian et al. 2019). Apart from that, *I. galbana* and *T. chui* achieved the highest accumulation during the log phase due to an active multiplication of cells. It is well noted that GSH plays a pivotal role in various biological processes, including the synthesis of proteins and nucleic acids (Sharma et al. 2012). Contrarily, the drop of GSH content in *I. galbana* and *T. chui* observed during the late phases might be correlated to the overproduction of ROS generation that weakened the GSH which would cease the inability of microalgae cells to function properly (Roy et al. 2021).

Correspondence analysis (CA) of the antioxidative responses of *C. vulgaris*, *I. galbana*, and *T. chui* at different growth phases.

Antioxidative mechanisms are generally interrelated, where a deficit in one of them will be supported by the overproduction of other antioxidants. Figure 6 summarises the antioxidative responses of microalgae *C. vulgaris*, *I. galbana*, and *T. chui* at different growth phases. It can be postulated that *C. vulgaris*, *I. galbana*, and *T. chui* possess different antioxidative responses throughout their entire growth phases. Non-enzymatic antioxidants of *C. vulgaris* mostly occurred at the mid-stationary phase, including Chls a & b, CAR, AsA, and total GSH, aside from higher activity of GPX. The early stationary phases are composed of enzymatic antioxidants comprising SOD, CAT, APX, and GPX, as well as a non-enzymatic TOC (Figure 6a). Similarly, most of the antioxidants in *I. galbana* were actively produced at the stationary phase (Figure 6b). There was no rise in antioxidant production during the death phase in *I. galbana*. Differing from *I. galbana*, *T. chui* consists of an abundance of antioxidants in the log and early stationary phases, including Chls a and b and TOC. On the other hand, the mid-stationary and death phases in *T. chui* revealed the identical ascending of APX and GPX, as well as AsA. Intriguingly, Chl b and AsA were persistently produced at the phases with the highest antioxidative responses, mid-stationary in *C. vulgaris*, early stationary in *I. galbana*, and lag to death-phases except for the log phase in *T. chui*. The different responses of all antioxidants in all three studied species throughout growth phases indicate that these antioxidants could work synergistically to minimise the impact of oxidative stress.

Conclusion

C. vulgaris, *I. galbana*, and *T. chui* exhibited typical growth phases i.e., lag, log, early, mid-stationary, and death phases. All microalgae species studied exhibited different biomass and antioxidative responses throughout the growth phases. The early stationary phase was identified as the critical period for significant increases in antioxidant levels, with α -tocopherol (TOC) reaching the highest production across all species. Additionally, CAT and GPX were most abundant in *C. vulgaris* and *I. galbana*, while SOD and APX peaked in *C. vulgaris* and *T. chui*. These findings suggest that the early stationary phase is optimal for harvesting microalgae for high antioxidant yields. By elucidating the dynamics of antioxidant production in various growth stages, these findings offer the potential to optimize cultivation conditions for enhanced antioxidant yield, which is pivotal for applications in health foods, nutraceuticals, and aquaculture. Future research



should focus on optimising other culture conditions, such as light intensity, temperature, nutrient concentration, and photoperiod, to maximise antioxidant production in microalgae. In addition, comparative studies with other microalgal species and strains can identify those microalgae with superior antioxidant production capabilities.

Competing interests The authors declare no competing interests.

Authors' contributions NY have made a substantial contribution to the concept and design of all the experiments, analysis, and interpretation of data for the article, as well as finalising the manuscript. NSY did all the experiments. MJ refined the writing style and language and helped finalise the manuscript. All authors read and approved the final manuscript.

Acknowledgements The authors wish to thank Universiti Malaysia Terengganu for funding this project (UMT/TAPE-RG-2021/55346). Not forgetting the research assistants and postgraduate and undergraduate students involved in this study.

References

- Agrawal R, Patwardhan MV (1993) Production of peroxidase enzyme by callus cultures of *Citrus aurantifolia* S. J Sci Food Agric 61(3):377-378
- Ahmad MT, Shariff M, Md. Yusoff F, Goh YM, Banerjee S (2020) Applications of microalga *Chlorella vulgaris* in aquaculture. Rev Aquac 12(1):328-346
- Ansari FA, Guldhe A, Gupta SK, Rawat I, Bux F (2021) Improving the feasibility of aquaculture feed by using microalgae. Environ Sci Pollut Res 28:43234-43257. <https://doi.org/10.1007/s11356-021-14989-x>
- Bauer LM, Costa JAV, da Rosa APC, Santos LO (2017) Growth stimulation and synthesis of lipids, pigments and antioxidants with magnetic fields in *Chlorella kessleri* cultivations. Bioresour Technol 244(2):425-432
- Belaidi FS, Salvagnac L, Souleille SA, Blatché MC, Bedel-Pereira E, Séguy I, Temple-Boyer P, Launay J (2020) Accurate physiological monitoring using lab-on-a-chip platform for aquatic micro-organisms growth and optimized culture. Sens Actuators B Chem 321:128492
- Bradford MM (1976) A rapid and sensitive method for the quantitation of microgram quantities of protein utilizing the principle of protein-dye binding. Anal Biochem 72(1):248-254
- Carlberg I, Mannervik B (1985) Glutathione reductase. Methods Enzymol 113:484-490
- Chatzikonstantinou M, Kalliampakou A, Gatzogia M, Fletmetakis E, Katharios P, Labrou NE (2017) Comparative analyses and evaluation of the cosmeceutical potential of selected *Chlorella* strains. J Appl Phycol 29(1):179-188
- Chen S, Zhang W, Li J, Yuan M, Zhang J, Xu F, Xu H, Zhang X, Wang L (2020) Ecotoxicological effects of sulfonamides and fluoroquinolones and their removal by a green alga (*Chlorella vulgaris*) and a cyanobacterium (*Chrysochloris ovalsporum*). Environ Pollut 263:114554
- Cheng J, Qiu H, Chang Z, Jiang Z, Yin W (2016) The effect of cadmium on the growth and antioxidant response for freshwater algae *Chlorella vulgaris*. SpringerPlus 5(1):1-8
- Chioccioli M, Hankamer B, Ross IL (2014) Flow cytometry pulse width data enables rapid and sensitive estimation of biomass dry weight in the microalgae *Chlamydomonas reinhardtii* and *Chlorella vulgaris*. PLoS One 9(5):e97269
- Chowdury KH, Nahar N, Deb UK (2020) The growth factors involved in microalgae cultivation for biofuel production: A review. CWEEE 9:185-215. <https://doi.org/10.4236/cweee.2020.94012>
- Claiborne A (1985) Catalase activity. In: Greenwald RA (ed.), CRC handbook of methods for oxygen radical research, CRC Press, Boca Raton
- Del Mondo A, Smerilli A, Sané E, Sansone C, Brunet C (2020) Challenging microalgal García JL, de Vicente M, Galán B (2017) Microalgae, old sustainable food and fashion nutraceuticals. Microb Biotechnol 10(5):1017-1024
- Giannuzzi L, Krock B, Minaglia MCC, Rosso L, Houghton C, Sedan D, Malanga G, Espinosa M, Andrinolo D, Hernando M (2016) Growth, toxin production, active oxygen species and catalase activity of *Microcystis aeruginosa* (Cyanophyceae) exposed to temperature stress. Comp Biochem Physiol C Pharmacol Toxicol Endocrinol 189:22-30. <https://doi.org/10.1016/j.cbpc.2016.07.001>
- Godbey WT (2021) Biotechnology and its applications: using cells to change the world, 2nd edn. Academic Press, London. <https://doi.org/10.1016/B978-0-12-817726-6.00005-8>
- Guillard RR (1975) Culture of phytoplankton for feeding marine invertebrates. In: Smith WL, Chanley MH (eds.), Culture of marine invertebrate animals. Springer, Boston, MA
- Hamed SM, Zinta G, Klöck G, Asard H, Selim S, AbdElgawad H (2017) Zinc-induced differential oxidative stress and antioxidant responses in *Chlorella sorokiniana* and *Scenedesmus acuminatus*. Ecotoxicol Environ Saf 140:256-263
- Hasanuzzaman M, Borhanuddin Bhuyan MHM, Parvin K, Bhuiyan TF, Anee TI, Nahar K, Hossen MS, Zulficar F, Alam MM, Fujita M (2020) ROS metabolism in plants under environmental stress: A review of recent experimental evidence. Int J Mol Sci:21:8695. <https://doi.org/10.3390/ijms21228695>
- Häubner N, Sylvander P, Vuori K, Snoeijs P (2014) Abiotic stress modifies the synthesis of alpha-tocopherol and beta-carotene in phytoplankton species. J Phycol 50(4):753-759
- Hu Q, Sommerfeld M, Jarvis E, Ghirardi M, Posewitz M, Seibert M, Darzins A (2008) Microalgal triacylglycerols as feedstocks for biofuel production: Perspectives and advances. Plant J 54(4):621-639
- Huang W, Ratkowsky DA, Hui C, Wang P, Su J, Shi P (2019) Leaf fresh weight versus dry weight: which is better for describing the scaling relationship between leaf biomass and leaf area for broad-leaved plants? Forests 10:256. <http://doi:10.3390/f10030256>
- Ismaiel MMS, El-Ayouty YM, Piercey-Normore M (2016) Role of pH on antioxidants production by *Spirulina (Arthrospira platensis)*. Braz J Microbiol 47(2):298-304
- Jaishankar J, Srivastava P (2017) Molecular basis of stationary phase survival and applications. Front Microbiol 8. <https://doi.org/10.3389/fmicb.2017.01281>



- org/10.3389/fmicb.2017.02000
- Janknegt PJ, De Graaff CM, Van de Poll WH, Visser RJ, Rijstenbil JW, Buma AG (2009) Short-term antioxidative responses of 15 microalgae exposed to excessive irradiance including ultraviolet radiation. *Eur J Phycol* 44(4):525-539
- Javier LH, Benzekri H, Gut M, Claros MG, van Bergeijk S, Cañavate JP, Manchado M (2018) Characterization of iodine-related molecular processes in the marine microalga *Tisochrysis lutea* (Haptophyta). *Front Mar Sci* 5:134
- Jin M, Xiao X, Qin L, Geng W, Gao Y, Li L, Xue J (2020) Physiological and morphological responses and tolerance mechanisms of *Isochrysis galbana* to Cr (VI) stress. *Bioresour Technol* 302:122860. <https://doi.org/10.1016/j.biortech.2020.122860>
- Kasan NA, Hashim FS, Haris N, Zakaria MF, Mohamed NN, Rasdi NW, Wahid MEA, Takahashi K, Jusoh M (2020) Isolation of freshwater and marine indigenous microalgae species from Terengganu water bodies for potential uses as live feeds in aquaculture industry. *Int Aquat Res* 12(1):74-83
- Khatoon H, Haris H, Rahman NA, Zakaria MN, Begum H, Mian S (2018) Growth, proximate composition and pigment production of *Tetraselmis chuii* cultured with aquaculture wastewater. *J Ocean U China* 17(3):641-646
- Kokkali M, Marti-Quijal FJ, Taroncher M, Ruiz MJ, Kousoulaki K, Barba FJ (2020) Improved extraction efficiency of antioxidant bioactive compounds from *Tetraselmis chuii* and *Phaeodoactylum tricorutum* using pulsed electric fields. *Molecules* 25(17):3921
- Kong W, Song H, Cao Y, Yang H, Hua S, Xia C (2011) The characteristics of biomass production, lipid accumulation and chlorophyll biosynthesis of *Chlorella vulgaris* under mixotrophic cultivation. *AJB* 10(55):11620-11630
- Manzoor MF, Afraz MT, Yilmaz BB, Adil M, Arshad N, Goksen G, Ali M, Zeng X (2024) Recent progress in natural seaweed pigments: green extraction, health-promoting activities, techno-functional properties and role in intelligent food packaging. *J Agric Res* 15:100991. <https://doi.org/10.1016/j.jafr.2024.100991>
- Mata TM, Martins AA, Caetano NS (2010) Microalgae for biodiesel production and other applications: a review. *Renew Sustain Energy Rev* 14:217–232
- Norhayati Y, Afzan AW, Jannah SSN, Nurul Wahidah MR (2016) Antioxidative responses of *Cocos nucifera* against infestation by the Red Palm Weevil (RPW), *Rhynchophorus ferrugineus*, a new invasive coconut pest in Malaysia. *Sains Malays* 45(7):1035-1040
- Paes CR, Faria GR, Tinoco NA, Castro DJ, Barbarino E, Lourenço SO (2016) Growth, nutrient uptake and chemical composition of *Chlorella* sp. and *Nannochloropsis oculata* under nitrogen starvation. *Lat Am J Aquat Res* 44(2):275-292
- Pokora W, Reszka J, Tukaj Z (2003) Activities of superoxide dismutase (SOD) isoforms during growth of *Scenedesmus* (Chlorophyta) species and strains grown in batch-cultures. *Acta Physiol Plant* 25(4):375-384
- Price AH, Taylor A, Ripley SJ, Griffiths A, Trewavas AJ, Knight MR (1994) Oxidative signals in tobacco increase cytosolic calcium. *The Plant Cell* 6(9):1301-1310
- Rahman NA, Katayama T, Wahid MEA, Kasan NA, Khatoon H, Yamada Y, Takahashi K (2020) Taxon-and growth phase-specific antioxidant production by chlorophyte, bacillariophyte and haptophyte strains isolated from tropical waters. *Front Bioeng Biotechnol* 8:1315
- Ramlee A, Rasdi NW, Abd Wahid ME, Jusoh M (2021) Microalgae and the factors involved in successful propagation for mass production. *J Sustain Sci Manage* 16:21-42
- Reitan KI, Øie G, Jørgensen H, Wang X (2021) Chemical composition of selected marine microalgae, with emphasis on lipid and carbohydrate production for potential use as feed resources. *J Appl Phycol* (33):3831-3842
- Ren HY, Xiao RN, Kong F, Zhao L, Xing D, Ma J, Ren NQ, Liu BF (2019) Enhanced biomass and lipid accumulation of mixotrophic microalgae by using low-strength ultrasonic stimulation. *Bioresour Technol* 272:606-610
- Rezayian M, Niknam V, Ebrahimzadeh H (2019) Oxidative damage and antioxidative system in algae. *Toxicol Rep* 6:1309-1313
- Roy UK, Nielsen BV, Milledge JJ (2021) Antioxidant production in *Dunaliella*. *Appl Sci* 11(9):3959
- Sahastrabudde AP (2016) Counting of RBC and WBC using image processing: a review. *Int J Res Eng Technol* 5(05):356-360
- Sairam RK, Shukla DS, Saxena DC (1997) Stress induced injury and antioxidant enzymes in relation to drought tolerance in wheat genotypes. *Biol Plant* 40(3):357-364
- Sharma P, Jha AB, Dubey RS, Pessarakli M (2012) Reactive oxygen species, oxidative damage and antioxidative defense mechanism in plants under stressful conditions. *J Bot* 2012(1):217037. <https://doi.org/10.1155/2012/217037>
- Sharma J, Sarmah P, Bishnoi NR (2020) Market perspective of EPA and DHA production from microalgae. In: Patel AK, Matsakas L (eds) *Nutraceutical fatty acids from oleaginous microalgae: A human health perspective*, Wiley, New York. <https://doi.org/10.1002/9781119631729.ch11>
- Shi TQ, Wang LR, Zhang ZX, Sun XM, Huang H (2020) Stresses as first-line tools for enhancing lipid and carotenoid production in microalgae. *Front Bioeng Biotechnol* 8(610):1-9
- Siddhath, Surasani VKR, Singh A, Singh SM, Hauzoukim L, Murthy N, Baraiya KG (2024) Bioactive compounds from micro-algae and its application in foods: a review. *Discover Food* 4:27. <https://doi.org/10.1007/s44187-024-00096-6>
- Sigaud-Kutner TCS, Pinto E, Okamoto OK, Latorre LR, Colepicolo P (2002) Changes in superoxide dismutase activity and photosynthetic pigment content during growth of marine phytoplankters in batch-cultures. *Physiol Plant* 114(4):566-571
- Singh G, Patidar SK (2018) Microalgae harvesting techniques: a review. *J Environ Manage* 217:499-508
- Su M, Bastiaens L, Verspreet J, Hayes M (2023) Applications of microalgae in foods, pharma and feeds and their use as fertilizers and biostimulants: legislation and regulatory aspects for consideration. *Foods* 12:3878. <https://doi.org/10.3390/foods12203878>
- Sun X, Zhong Y, Huang Z, Yang Y (2014) Selenium accumulation in unicellular green alga *Chlorella vulgaris* and its effects on antioxidant enzymes and content of photosynthetic pigments. *PLoS One* 9(11):e112270. <https://doi.org/10.1371/journal.pone.0112270>
- Torres PB, Chow F, Furlan CM, Mandelli F, Mercadante A, Santos DYACD (2014) Standardization of a protocol to extract and analyze chlorophyll a and carotenoids in *Gracilaria tenuistipitata* Var. Liu. Zhang and Xia (Rhodophyta). *Braz J Oceanogr* 62(1):57-63
- Udayan A, Pandey AK, Sirohi R, Sreekumar N, Sang BI, Sim SJ, Kim SH, Pandey A (2023) Production of microalgae with high lipid content and their potential as sources of nutraceuticals. *Phytochem Rev* 22:833–860. <https://doi.org/10.1007/s11101-021-09784-y>
- Ugya AY, Imam TS, Li A, Ma J, Hua X (2019) Antioxidant response mechanism of freshwater microalgae species to reactive oxygen species production: a mini review. *Chem Ecol* 36(2):174-193



- Zachleder V, Ivanov IN, Kselíková V, Bialevich V, Vítová M, Ota S, Takeshita T, Kawano S, Bišová K (2021) Characterization of growth and cell cycle events affected by light intensity in the green alga *Parachlorella kessleri*: a new model for cell cycle research. *Biomolecules* 11(6). <https://doi.org/10.3390/biom11060891>
- Zhang S, He Y, Sen B, Wang G (2020) Reactive oxygen species and their applications toward enhanced lipid accumulation in oleaginous microorganisms. *Bioresour Technol* 307:123234. <https://doi.org/10.1016/j.biortech.2020.123234>

Publisher's Note

IAU remains neutral with regard to jurisdictional claims in published maps and institutional affiliations.

